

Tunable erbium-doped microbubble laser fabricated by sol-gel coating

YONG YANG,^{1,2,*} FUCHUAN LEI,¹ SHO KASUMIE,¹ LINHUA XU,³
JONATHAN M. WARD,¹ LAN YANG,³ AND SÍLE NIC CHORMAIC¹

¹*Light-Matter Interactions Unit, Okinawa Institute of Science and Technology Graduate University, Onna, Okinawa 904-0495, Japan*

²*National Engineering Laboratory for Fiber Optics Sensing Technology, Wuhan University of Technology, Wuhan, 430070, China*

³*Department of Electrical and Systems Engineering, Washington University, St. Louis, Missouri 63130, USA*

*yong.yang@oist.jp

Abstract: In this work, we show that the application of a sol-gel coating renders a microbubble whispering gallery resonator into an active device. During the fabrication of the resonator, a thin layer of erbium-doped sol-gel is applied to a tapered microcapillary, then a microbubble with a wall thickness of 1.3 μm is formed with the rare earth ions diffused into its wall. The doped microbubble is pumped at 980 nm and lases in the emission band of the Er^{3+} ions at 1535 nm. The laser wavelength can be shifted by aerostatic pressure tuning of the whispering gallery modes of the microbubble. Up to 240 pm tuning is observed with 2 bar of applied pressure. We also show that the doped microbubble could be used as a compact, tunable laser source.

© 2016 Optical Society of America

OCIS codes: (140.3600) Lasers, tunable; (140.3500) Lasers, erbium; (140.3948) Microcavity devices; (280.5475) Pressure measurement.

References and links

1. T. Aoki, B. Dayan, E. Wilcut, W. P. Bowen, A. S. Parkins, T. J. Kippenberg, K. J. Vahala, and H. J. Kimble, "Observation of strong coupling between one atom and a monolithic microresonator." *Nature* **443**, 671–674 (2006).
2. M. Aspelmeyer, T. J. Kippenberg, and F. Marquardt, "Cavity optomechanics," *Reviews of Modern Physics* **86**, 1391–1452 (2014).
3. R. Madugani, Y. Yang, J. M. Ward, V. H. Le, and S. Nic Chormaic, "Optomechanical transduction and characterization of a silica microsphere pendulum via evanescent light," *Appl. Phys. Lett.* **106**, 241101 (2015).
4. D. V. Strekalov, C. Marquardt, A. B. Matsko, H. G. L. Schwefel, and G. Leuchs, "Nonlinear and Quantum Optics with Whispering Gallery Resonators," arXiv p. 1605.07972 (2016).
5. M. R. Foreman, J. D. Swaim, and F. Vollmer, "Whispering gallery mode sensors," *Advances in Optics and Photonics* **7**, 168 (2015).
6. J. M. Ward, N. Dhasmana, and S. Nic Chormaic, "Hollow core, whispering gallery resonator sensors," *The European Physical Journal Special Topics* **223**, 1917–1935 (2014).
7. V. Sandoghdar, F. Treussart, J. Hare, V. Lefèvre-Seguin, J. M. Raimond, and S. Haroche, "Very low threshold whispering-gallery-mode microsphere laser," *Physical Review A* **54**, R1777–R1780 (1996).
8. Z. Cai, H. Xu, G. Stéphan, P. Féron, and M. Mortier, "Red-shift in Er:ZBLALiP whispering gallery mode laser," *Optics Communications* **229**, 311–315 (2004).
9. J. M. Ward and S. Nic Chormaic, "Thermo-optical tuning of whispering gallery modes in Er:Yb co-doped phosphate glass microspheres," *Appl. Phys. B* **100**, 847 (2010).
10. L. He, a. K. Özdemir, and L. Yang, "Whispering gallery microcavity lasers," *Laser & Photonics Reviews* **7**, 60–82 (2013).
11. L. Yang and K. J. Vahala, "Gain functionalization of silica microresonators," *Optics Letters* **28**, 592 (2003).
12. M. Ferrari, A. Chiasera, E. Moser, Y. Jestin, G. Nunzi Conti, S. Berneschi, G. Righini, S. Soria, M. Brenci, F. Cosi, C. Armellini, A. Chiappini, L. Ghisa, S. Trebaol, Y. Dumeige, S. Pelli, and P. Féron, "Glass microspherical lasers," *Advances in Science and Technology* **55**, 46–55 (2009).
13. L. Yang, T. Carmon, B. Min, S. M. Spillane, and K. J. Vahala, "Erbium-doped and Raman microlasers on a silicon chip fabricated by the sol gel process," *Applied Physics Letters* **86**, 091114 (2005).
14. L. He, S. K. Ozdemir, J. Zhu, W. Kim, and L. Yang, "Detecting single viruses and nanoparticles using whispering gallery microlasers," *Nature Nanotechnology* **6**, 428–432 (2011).
15. B. Peng, a. K. Özdemir, F. Lei, F. Monifi, M. Gianfreda, G. L. Long, S. Fan, F. Nori, C. M. Bender, and L. Yang, "Parity time-symmetric whispering-gallery microcavities," *Nature Physics* **10**, 394–398 (2014).

16. F. Lei, B. Peng, a. K. Özdemir, G. L. Long, and L. Yang, "Dynamic Fano-like resonances in erbium-doped whispering-gallery-mode microresonators," *Applied Physics Letters* **105**, 101112 (2014).
17. X.-F. Jiang, C.-L. Zou, L. Wang, Q. Gong, and Y.-F. Xiao, "Whispering-gallery microcavities with unidirectional laser emission," *Laser & Photonics Reviews* **10**, 40–61 (2016).
18. M. Sumetsky, Y. Dulashko, and R. S. Windeler, "Optical microbubble resonator," *Optics letters* **35**, 898–900 (2010).
19. A. Watkins, J. Ward, Y. Wu, and S. Nic Chormaic, "Single-input spherical microbubble resonator," *Optics letters* **36**, 2113–2115 (2011).
20. M. Li, X. Wu, L. Liu, and L. Xu, "Kerr parametric oscillations and frequency comb generation from dispersion compensated silica micro-bubble resonators," *Optics express* **21**, 16908–13 (2013).
21. Y. Yang, Y. Ooka, R. Thompson, J. Ward, and S. Nic Chormaic, "Degenerate four-wave-mixing in a silica hollow bottle-like microresonator," *Opt. Lett.* **41**, 575 (2016).
22. I. M. White, H. Oveys, and X. Fan, "Liquid-core optical ring-resonator sensors," *Optics Letters* **31**, 1319 (2006).
23. R. Henze, T. Seifert, J. Ward, and O. Benson, "Tuning whispering gallery modes using internal aerostatic pressure," *Optics Letters* **36**, 4536–4538 (2011).
24. Y. Yang, S. Saurabh, J. M. Ward, and S. Nic Chormaic, "High-Q, ultrathin-walled microbubble resonator for aerostatic pressure sensing," *Optics Express* **24**, 294 (2016).
25. G. Bahl, K. H. Kim, W. Lee, J. Liu, X. Fan, and T. Carmon, "Brillouin cavity optomechanics with microfluidic devices," *Nature Communications* **4**, 1994 (2013).
26. W. Lee, Y. Sun, H. Li, K. Reddy, M. Sumetsky, and X. Fan, "A quasi-droplet optofluidic ring resonator laser using a micro-bubble," *Applied Physics Letters* **99**, 091102 (2011).
27. Y.-C. Chen, Q. Chen, and X. Fan, "Lasing in blood," *Optica* **3**, 809–815 (2016).
28. X. Fan and S.-H. Yun, "The potential of optofluidic biolasers," *Nature Methods* **11**, 141–147 (2014).
29. J. M. Ward, Y. Yang, and S. Nic Chormaic, "Glass-on-Glass Fabrication of Bottle-Shaped Tunable Microlasers and their Applications," *Scientific Reports* **6**, 25152 (2016).
30. C. Grivas, C. Li, P. Andreakou, P. Wang, M. Ding, G. Brambilla, L. Manna, and P. Lagoudakis, "Single-mode tunable laser emission in the single-exciton regime from colloidal nanocrystals," *Nat. Commun.* **4**, 2376 (2013).
31. V. D. Ta, R. Chen, and H. D. Sun, "Tuning whispering gallery mode lasing from self-assembled polymer droplets," *Scientific Reports* **3**, 1362 (2013).
32. W. Lee, H. Li, J. D. Suter, K. Reddy, Y. Sun, and X. Fan, "Tunable single mode lasing from an on-chip optofluidic ring resonator laser," *Applied Physics Letters* **98**, 061103 (2011).
33. R. Madugani, Y. Yang, V. H. Le, J. M. Ward, and S. Nic Chormaic, "Linear laser tuning using a pressure-sensitive microbubble resonator," *IEEE Photonics Technology Letters* **28**, 1134–1137 (2016).

1. Introduction

Whispering gallery mode resonators (WGR) are traveling wave resonators, which can have ultra-high quality (Q) factors and relatively small mode volumes. Due to these features, recently WGRs have been used for research areas as diverse as cavity quantum electrodynamics (cQED) [1], optomechanics [2, 3], nonlinear optics [4] and sensing [5, 6]. Very high Q, low threshold WGR microlasers can be realized when the resonator is made from a material with gain [7–9]. For this purpose, many fabrication methods have been developed [10], one of which is the sol-gel wet chemical synthesis technique. Rare earth ions are mixed into the sol-gel precursor solution and, based on the hydrolysis and condensation reactions of metal-alkoxide precursors in aqueous solutions, alcohol, or other media, a silica film can be formed with the gain medium. Microlasers made from sol-gel coated microspheres [11, 12] and microtoroids [13] have already been realized. Such active WGRs are used for applications such as nanoparticle sensing [14] and fundamental physics research [15–17]. Sol-gel is a low-cost, flexible way to functionalize a WGR and can also be applied to microbubble resonators (MBR) as we shall discuss in the following.

MBRs are a more recently developed geometry of WGRs [6, 18, 19] that are hollow, while still maintaining a high Q-factor and small mode volume. Similar to WGRs, MBRs can also be used in a wide variety of applications, such as nonlinear optics [20, 21], sensing [22–24], and optomechanics [25]. Active MBRs have also been developed by injecting dye solution [26, 27] or other bio-chemical liquids [28] into the core of the resonator such that lasing emission can be achieved. In order to achieve lasing from the wall instead of the core, a glass-on-glass wetting technique was developed [29], whereby bulk Er-doped glass was melted onto the surface of a microcapillary. The wall thickness is limited in this method. To fabricate an MBR with thinner

gain activated wall and to improve the attainable sensitivity, alternative methods need to be found.

In this work, a sol-gel coating technique is used to introduce Er^{3+} ions into the wall of an MBR and lasing in the 1550 nm band is realized. With a subwavelength wall thickness, the lasing is tuned by applying internal aerostatic pressure to the wall of the resonator. Temperature [8, 9, 30] and mechanical [31] tuning of laser sources based on WGRs have been reported previously. Refractive index tuning of the laser have been demonstrated [32] in a dye solution filled MBR. Here, the MBR laser is tuned by pressure without any gain medium in the core.

2. Fabrication

Having a high Q cavity mode is a necessary precondition for achieving low threshold lasing. For a passive MBR, we have previously demonstrated that the Q-factor can reach 10^7 , close to the theoretical limit [24]. To maintain the high-Q after introducing a gain medium, we dissolved erbium ions into a sol-gel precursor solution and used this as the gain material, ensuring that the erbium ions are distributed uniformly in the silica matrix of the MBR after fabrication. The sol-gel precursor solution was made by mixing erbium(III) nitrate hydrate (i.e. $\text{Er}(\text{NO}_3)_3 \cdot 5\text{H}_2\text{O}$), tetraethoxysilane (i.e. TEOS), isopropyl alcohol (i.e. IPA), water (H_2O), and hydrochloric acid (37% HCl) with a weight ratio of 0.03:6.5:6.1:0.7:0.6 for 2 hours at 70°C [11]. After 24 hours, the sol-gel precursor was ready to use.

The fabrication of the erbium-doped MBR is presented in Fig.1. First, two counter-propagating CO_2 laser beams were focused onto a silica capillary (outer diameter $350\ \mu\text{m}$, inner diameter $250\ \mu\text{m}$) to heat it, thereby allowing us to pull the capillary into a uniform taper with a waist diameter of around $30\ \mu\text{m}$. Afterwards, a droplet of the sol-gel precursor was transferred to the tapered capillary. Finally, the capillary was filled with compressed air and the CO_2 laser was reapplied to reheat it. With the correct choice of laser power, the section of capillary in the focus of the laser beams expands to form a MBR. Due to the high temperature, the residual sol-gel solvent was removed and only silica doped with erbium ions remained; this material formed the wall of the MBR during the expansion process. The maximum erbium concentration was $5 \times 10^{19}/\text{cm}^3$ according to the concentration in the sol-gel precursor.

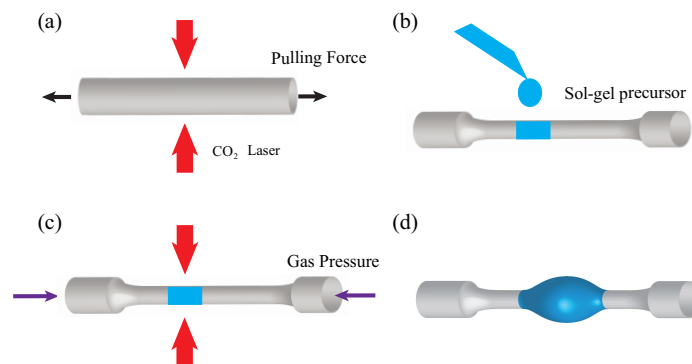


Fig. 1. Schematic of the fabrication process for a sol-gel coated MBR using CO_2 laser heating. (a) A capillary is tapered using a CO_2 laser heat source. (b) Erbium ions are dissolved into a sol-gel precursor, which is drop-coated onto the tapered capillary. (c-d) The CO_2 laser heats the sol-gel and internal air pressure is applied until a MBR is formed.

3. Aero-pressure tuning of the MBR laser

3.1. Experimental setup

The MBR was coupled to a tapered optical fiber in contact. The laser source was a broadband, 980 nm laser with a maximum power of 200 mW. The tapered fiber waist was about $1.1 \mu\text{m}$. Since the 980 pump has a linewidth of about 2 nm, even without fine tuning of the pump laser frequency, some coupling into the MBR modes can occur. About 10% of the pump power was absorbed after passing the MBR. The coupled laser power excited 1535 nm lasing in the Er ions. The experimental setup is illustrated in Fig. 2. The MBR was placed in a dry nitrogen gas environment to maintain the optical quality. In order to tune the frequency of the MBR, one output of the MBR was sealed with epoxy, while the other end was connected to a compressed air cylinder. The internal pressure of the MBR was adjustable via a valve and the pressure reading was recorded on a pressure gauge. During the experiment, the pressure was varied from 0 bar to 2.5 bar. The lasing spectrum was measured on an optical spectrum analyzer (OSA), which had a minimum resolution of 0.07 nm.

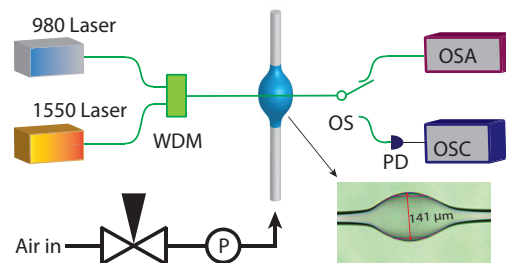


Fig. 2. Schematic of the setup for pressure tunable lasing in an MBR. P: pressure gauge; OS: optical switch; PD: photo detector; OSC: oscilloscope; OSA: optical spectrum analyzer. The inset shows a microscopic image of the sol-gel coated MBR. The diameter of the MBR is $141 \mu\text{m}$.

3.2. Experimental results

First, the lasing threshold for the coated MBR was measured. The pump power was adjusted from 17.9 mW to 94.7 mW. Because the pump is broadband, it is difficult to know exactly how much power couples into the modes; therefore, we used the total pump power to evaluate the threshold. The laser output power at 1535.66 nm was recorded against the pump power and is plotted in Fig. 3(a), the threshold is estimated to be about 27 mW. From the fluorescence background (see Fig. 3(b)) single mode lasing occurs (see Fig. 3(c)) when the pump power is beyond the threshold. In reality, the actual threshold should be significantly lower than this upper limit due to coupling losses.

By applying aerostatic pressure inside the bubble, the MBR expands so that all modes are red-shifted [23]. With a maximum applied pressure of 2.5 bar, the laser emission at 1535 nm was shifted by about 240 pm, as shown in Fig. 4(a). The shift of the modes is much smaller than the bandwidth of the pump. Therefore, even without tuning the wavelength of the pump, modes can still be excited via the 980 nm source. In the case here, single mode lasing was achieved within the pressure tuning range. The wavelength shift as a function of the applied pressure is plotted in Fig. 4(b). Note that this measurement is not so accurate since the laser linewidth and the mode shifts are smaller than the resolution of the OSA. However, a linear relationship is still obvious, similar to the linear tuning property of the modes of a passive MBR [23]. The sensitivity is the slope of the pressure tuning curve, which ranges from approximately 6 GHz/bar to 14 GHz/bar, as determined by the error bars in Fig. 4(b).

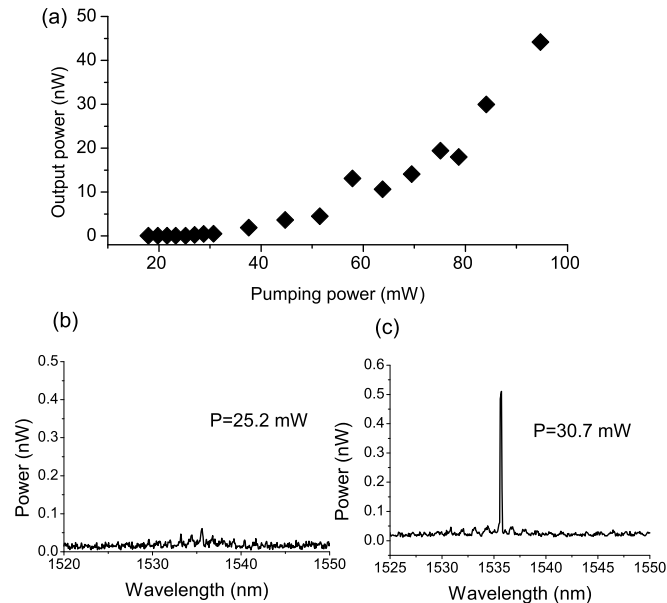


Fig. 3. (a) Lasing threshold measurement of a sol-gel coated MBR. The total power of the pump laser is used for estimation. The threshold is about 27 mW for the pump laser. (b) The spectrum with the pump power below threshold. (c) The single mode lasing spectrum near the threshold.

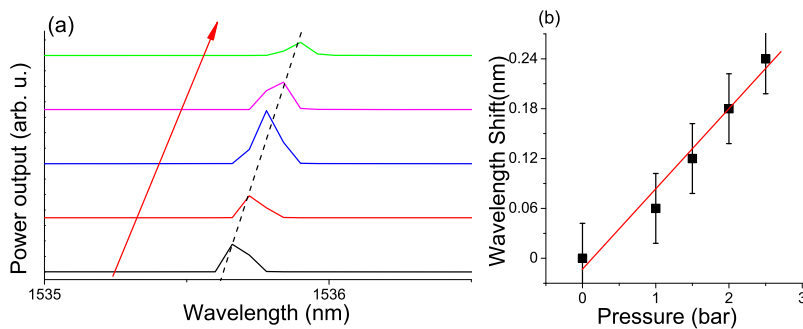


Fig. 4. (a) The laser spectrum of the sol-gel coated MBR at different pressures. The arrow shows the direction of the pressure increase. From the bottom to the top are the laser emission lines from 0 bar to 2.5 bar applied pressure. The resolution of the spectrum is limited by the OSA. (b) The wavelength shift of the lasing mode as a function of the applied pressure. The red line is a linear fit and the error bar is set by the resolution of the OSA.

In order to obtain a more accurate pressure tuning slope, we measured the transmission spectrum by switching to a finely tunable laser, around 1535 nm (New focus Velocity 6728), and a photodetector connected to an oscilloscope, as shown in Fig. 2. The transmission spectra of this MBR laser, for different applied pressures, are given in Fig. 5(a), the mode is indicated by an arrow and the measured Q-factor is about 10^6 . The resolution of the pressure tuning, measured by monitoring the pump transmission through the fiber coupler, was limited only by the Q-factor [24] and is, more accurate than measurements made using the spectrum analyzer. By tracking the resonance positions, shown in Fig. 5(b), a tuning sensitivity of 8.2 GHz/bar was

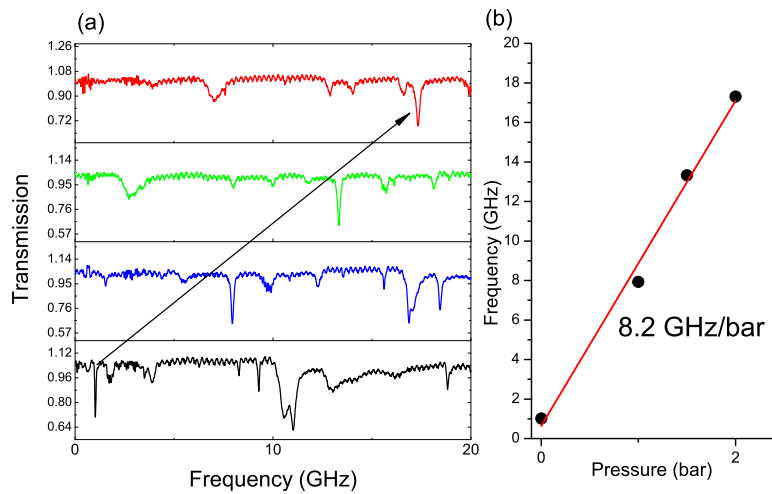


Fig. 5. (a) The transmission spectra at 1535.66 nm for different pressure. From the bottom to the top are transmission spectra at 0, 1, 1.5, 2 bar, respectively. The arrow shows the direction of the WGM shift due to the increase of the internal pressure. (b) Pressure tuning sensitivity fitted from the transmission spectra.

measured. From the microscope image of the MBR, the wall thickness of the MBR was estimated to be about $1.3 \mu\text{m}$. For an MBR with a diameter of $141 \mu\text{m}$, the obtainable sensitivity is calculated to be 8.5 GHz/bar [23], which is in accordance with the measured results.

4. Conclusion

By using a sol-gel technique, a layer of Er^{3+} ions was coated onto the outer surface of a MBR. We achieved lasing emission at 1535.66 nm when pumped at 980 nm. A pressure tunable laser was also demonstrated with a tuning range of 240 pm. This provides an alternative way of achieving a compact, WGR-based tunable laser source instead of the usual temperature tuning. The pressure tunable laser is expected to have improved tuning performance since pressure tuning is linear with good long term stability [33]. The lasing threshold can be further optimized if a narrow linewidth tunable pump laser is used. However, when the MBR is tuned, all modes including modes at the pump wavelength will shift. Therefore, a narrow band pump is not so practical for implementing such a tunable laser as the pump itself needs to be locked to the MBR mode. With broad band pumping, the laser remains coupled to the MBR mode, making the setup simple. Other rare earth ions can be diffused into the wall of the MBR thereby expanding the wavelength of the MBR laser to the visible range, and into the transparency window for aquatic fillings in the core. The linewidth of the lasing modes in an active MBR are narrower than modes in a passive MBR, and the reduced linewidth could improve the limit of detection for sensing applications [14].

Funding

Okinawa Institute of Science and Technology Graduate University; National Science Foundation (NSF) (1433311).